Biochimica et Biophysica Acta 1813 (2011) 704–712

Contents lists available at ScienceDirect

Biochimica et Biophysica Acta

journal homepage: www.elsevier.com/locate/bbamcr

2,3,7,8-Tetrachlorodibenzo-*p*-dioxin impairs iron homeostasis by modulating iron-related proteins expression and increasing the labile iron pool in mammalian cells

Rita Santamaria [a,*], Filomena Fiorito [b], Carlo Irace [a], Luisa De Martino [b], Carmen Maffettone [a], Giovanna Elvira Granato [b], Antonio Di Pascale [a], Valentina Iovane [b], Ugo Pagnini [b], Alfredo Colonna [a]

[a] *Dipartimento di Farmacologia Sperimentale, Università degli Studi di Napoli "Federico II", via D. Montesano 49, I-80131 Naples, Italy*
[b] *Dipartimento di Patologia e Sanità Animale, Università degli Studi di Napoli "Federico II", via F. Delpino 1, I-80137 Naples, Italy*

ARTICLE INFO

Article history:
Received 9 July 2010
Received in revised form 31 January 2011
Accepted 2 February 2011
Available online 17 February 2011

Keywords:
2,3,7,8-Tetrachlorodibenzo-*p*-dioxin
Iron metabolism
Iron-related proteins
Iron regulatory proteins
Labile iron pool

ABSTRACT

Cellular iron metabolism is essentially controlled by the binding of cytosolic iron regulatory proteins (IRP1 or IRP2) to iron-responsive elements (IREs) located on mRNAs coding for proteins involved in iron acquisition, utilization and storage. The 2,3,7,8-tetrachlorodibenzo-*p*-dioxin (TCDD) is one of the most potent toxins of current interest that occurs as poisonous chemical in the environment. TCDD exposure has been reported to induce a broad spectrum of toxic and biological responses, including significant changes in gene expression for heme and iron metabolism associated with liver injury. Here, we have investigated the molecular effects of TCDD on the iron metabolism providing the first evidence that administration of the toxin TCDD to mammalian cells affects the maintenance of iron homeostasis. We found that exposure of Madin–Darby Bovine Kidney cell to TCDD caused a divergent modulation of IRP1 and IRP2 RNA-binding capacity. Interestingly, we observed a concomitant IRP1 down-regulation and IRP2 up-regulation thus determining a marked enhancement of transferrin receptor 1 (TfR-1) expression and a biphasic response in ferritin content. The changed ferritin content coupled to TfR-1 induction after TCDD exposure impairs the cellular iron homeostasis, ultimately leading to significant changes in the labile iron pool (LIP) extent. Since important iron requirement changes occur during the regulation of cell growth, it is not surprising that the dioxin-dependent iron metabolism dysregulation herein described may be linked to cell-fate decision, supporting the hypothesis of a central connection among exposure to dioxins and the regulation of critical cellular processes.

1. Introduction

Many proteins that carry out fundamental cellular processes, including DNA synthesis and ATP production, require iron to function. Consequently, cellular iron deficiency abrogates the activity of iron-dependent proteins causing cellular growth arrest and death [1]. Conversely, iron excess is toxic because ferrous iron reacts with hydrogen peroxides or lipid peroxides to generate hydroxyl or lipid radicals, respectively. In turn, these radicals damage lipids membrane, proteins, and nucleic acids [2,3]. Thus, iron homeostasis must be tightly controlled at both systemic and cellular levels. The peptide hormone hepcidin is the master regulator of the systemic iron metabolism and is predominantly expressed in the liver [4,5]. Hepcidin modulates iron availability by promoting the internalization and degradation of the cellular iron exporter ferroportin 1, thus controlling the use of iron in organs. Cellular iron homeostasis is achieved by the coordinated expression of proteins involved in iron uptake, export, storage, and utilization [6]. The post-transcriptional control mediated by the iron regulatory proteins (IRPs) has emerged as central and essential [7–10]. In fact, the binding of IRP1 or IRP2 to cis-acting mRNA motifs termed iron-responsive elements (IREs) regulates the expression of proteins involved in iron acquisition, such as transferrin receptor 1 (TfR-1) [11] and divalent metal transporter 1 (DMT-1) [12] and storage, such as ferritin [13]. In particular, the IRPs binding to IRE on respective mRNAs represses ferritin protein synthesis and stabilizes the mRNAs of TfR-1 and DMT-1, promoting their translation. IRP1, the cytosolic counterpart of mitochondrial aconitase [14], is a bifunctional protein that, through [4Fe-4S] cluster assembly/disassembly, shifts from the aconitase to the

Abbreviations: TCDD, 2,3,7,8-tetrachlorodibenzo-*p*-dioxin; IRPs, iron regulatory proteins; IRE, iron-responsive element; TfR-1, transferrin receptor 1; DMT-1, divalent metal transporter 1; MDBK, Madin–Darby Bovine Kidney cells; MTT, 3-(4,5-dimethyl-2-thiazolyl)-2,5-diphenyl-2H-tetrazolium bromide; LIP, labile iron pool; SIH, salicylaldehyde isonicotinoyl hydrazone; 2-ME, 2-mercaptoethanol; CA-AM, calcein-acetomethoxy

* Corresponding author at: Department of Experimental Pharmacology, University of Naples, via D. Montesano, 49-80131, Naples, Italy. Tel.: +39 081 678421; fax: +39 081 678403.
E-mail address: rsantama@unina.it (R. Santamaria).

0167-4889/$ – see front matter © 2011 Elsevier B.V. All rights reserved.
doi:10.1016/j.bbamcr.2011.02.003

IRP1 form, mainly in response to the intracellular iron level. IRP2 lacks in the [4Fe-4S] cluster and its stability is controlled by an iron-regulated E3 ubiquitin ligase [15,16]. Consequently, the cytosolic free iron (labile iron pool, LIP) regulates RNA-binding capacity of IRP1 or induces IRP2 degradation. The IRPs RNA-binding activity is also regulated by other exogenous and endogenous factors, such as oxidative stress [17], nitric oxide signaling [18], protein phosphorylation [19], hypoxia/reoxygenation [20,21], viral infections [22], estrogens [23] as well as oxalomalic acid, an inhibitor of IRP1/c-acon [24–26].

Most recently, mechanism by which xenobiotics such as polychlorinated dibenzo-*p*-dioxins (PCDDs) and by-products, exert their biological and/or toxic effects have been the subject of intense investigations. The 2,3,7,8-tetrachlorodibenzo-*p*-dioxin (TCDD) is one of the most potent toxins that occur as poisonous chemicals in the environment [27]. In the last years, higher levels of TCDD were detected in pasturage areas and in milk samples from several farm animals collected in some areas of Campania Region (South Italy) [28,29]. Dietary ingestion is considered the primary source of general population exposure to TCDD. A major cause of concern related to exposure to dioxin-like compounds is their possible carcinogenicity in humans. Various molecular mechanisms have been suggested to be active in tumor induction by TCDD, and it is actually considered to act as a cancer promoter [30,31]. Besides being carcinogenic, dioxins induce a broad spectrum of toxic and biological responses in the reproductive and immune systems, including interference with endocrine system functions, immune suppression, teratogenicity, and hepatotoxicity [32–34].

Most of the biological effects of dioxins are linked to the aryl hydrocarbon receptor (AhR) activation [35,36]. The AhR is a key member of a transcription factor superfamily involved in the altered expression of target genes that results from exposure to dioxins. Recently, it has been reported that AhR functions as a ligand-dependent E3 ubiquitin ligase of certain nuclear receptors [37], such as the estrogen and androgen receptors. Besides the response to chemicals and pollutants, experimental evidence demonstrates that AhR also possesses physiological functions in crosstalk with other transcription factors that are independent of exogenous chemical exposure [38]. The binding of TCDD to the AhR and subsequent changes in gene expression have been studied intensively, but the mechanisms by which these lead to toxicity are still unclear. Interestingly, TCDD has been shown to interfere with the homeostasis of some cations and oligoelements, as well as iron metabolism [39,40]. In fact, it was demonstrated that iron potentiates both the hepatic porphyria and toxicity of TCDD in susceptible mice in an oxidative process with disturbance of iron regulatory protein activity [41]. Moreover, significant changes in genes expression for heme metabolism and iron homeostasis associated with liver injury were found in mice exposed for either 2 or 5 weeks to TCDD [42].

However, to our knowledge, no study has hitherto examined thoroughly the influence of TCDD in the maintenance of iron homeostasis. Hence, within a research project aimed to investigate the dioxin effects on cattle, we have evaluated the molecular effects of TCDD on the iron metabolism using an epithelial-like cell line, Madin–Darby Bovine Kidney (MDBK), a useful and standardized *in vitro* model for studying TCDD exposure in mammalian cells [43–45]. In particular, we have focused on the possible impact of this dioxin isomer in the expression and activity of the main cellular proteins involved in iron metabolism.

2. Materials and methods

2.1. Cell cultures and TCDD treatment

Madin–Darby Bovine Kidney (MDBK) cells (CCL22, American Type Culture Collection) were cultured in Dulbecco's modified Eagle's minimal essential medium (DMEM), supplemented with 2% fetal calf serum, 1% L-glutamine, 1% penicillin/streptomycin, 0.2% sodium pyruvate and 0.1% tylosin. All cultures were maintained in an incubator at 37 °C (in 5% CO_2/95% air).

Confluent cultures were exposed to different concentrations of TCDD (0.01, 1, 100 pg/ml) for 1, 12, 24, 48, 72 h. For iron repletion–depletion experiments, cells were treated with 50 μg/ml ferric ammonium citrate (FAC) or with 100 μM desferrioxamine (DFO) (Desferal, Novartis, Origgio, Varese, Italy) in growth medium for 18 h. 2,3,7,8-Tetrachlorodibenzo-*p*-dioxin (TCDD) in toluene was purchased from Supelco (St. Louis, MO). The original TCDD concentration was 10 μg/ml, and it was initially diluted to give a 10,000 pg/ml stock solution by mixing with DMEM. This stock solution was then diluted to give working solutions of 0.01, 1 and 100 pg/ml in DMEM, which were added to cultures. All other chemicals were of the highest purity that is commercially available.

2.2. Cell viability and proliferation

Cell viability was evaluated by MTT assay. The principle of this method is that 3-(4,5-dimethyl-2-thiazolyl)-2,5-diphenyl-2 H-tetrazolium bromide (MTT), a soluble tetrazolium salt, is converted to insoluble formazan by active mitochondrial dehydrogenases of living cells. Such conversion from yellowish soluble tetrazolium to purple formazan can be assayed spectrofluorimetrically. MDBK cells (2×10^4 cells/well), in 96-well plates, at confluency, were exposed to TCDD (0.01, 1, or 100 pg/ml) and incubated for 12, 24 and 48 h. MTT (5 mg/ml) was added to cells and after further 4 h of incubation, the medium was removed and replaced with DMSO to solubilize the MTT formazan crystals. The spectrophotometer absorbance at 570 nm was determined. Data are calculated as a percentage of the control, and results are the mean ± SEM of four independent experiments performed in duplicate.

To evaluate cell proliferation, MDBK cells (30×10^4 cells/flask) were plated in 25 cm^2 flask and, after reaching the confluence, were exposed to TCDD (0.01, 1, and 100 pg/ml) and incubated for 12, 24, or 48 h. At different times of incubation, adherent cells, removed from the culture substrate by treatment with trypsin–EDTA solution, were mixed with cells previously collected by centrifugation in supernatant from the same flask and resuspended at an adequate concentration in PBS. Thus, the entire cell population of the culture was reconstituted for determination of the cell number by counting them in a Burker chamber. Data are expressed as a percentage of the control, and results are the mean ± SEM of four independent experiments performed in duplicate.

2.3. Preparation of cellular extracts

After different times of incubation with TCDD, MDBK cells were washed and scraped off with PBS containing 1 mM EDTA. To obtain cytosolic extracts for electrophoretic mobility shift assay (EMSA), cells were treated with lysis buffer containing 10 mM HEPES, pH 7.5, 3 mM $MgCl_2$, 40 mM KCl, 5% (v/v) glycerol, 1 mM dithiothreitol (DTT), 0.2% (v/v) Nonidet P-40 (NP-40) and protease inhibitor tablets (Roche, Mannheim, Germany) at 4 °C. Cell debris and nuclei were pelleted by centrifugation at 15,000 × *g* for 10 min at 4 °C, and supernatants were stored at −80 °C. For Western blot analysis, cells were collected by scraping and low-speed centrifugation. Cell pellets were lysed at 4 °C for 30 min in a buffer containing 20 mM Tris–HCl, pH 7.4, 150 mM NaCl, 5 mM EDTA, 5% (v/v) glycerol, 10 mM NP-40 and protease inhibitor tablets (Roche). The supernatant fraction was obtained by centrifugation at 15,000 × *g* for 10 min at 4 °C and then stored at −80 °C. Protein concentration was determined by the Bio-Rad protein assay (Bio-Rad, Milan, Italy).

2.4. Electrophoretic mobility-shift assay (EMSA)

Plasmid pSPT-fer containing the sequence corresponding to the IRE of the H-chain of human ferritin, linearized at the BamHI site, was

transcribed in vitro as previously described [46]. For RNA–protein band-shift analysis, cytosolic extracts (5 μg) were incubated for 30 min at room temperature with 0.2 ng of in vitro transcribed ^{32}P-labelled IRE RNA. The reaction was performed in buffer containing 10 mM HEPES, pH 7.5, 3 mM $MgCl_2$, 40 mM KCl, 5% (v/v) glycerol, 1 mM DTT and 0.07% (v/v) NP-40, in a final volume of 20 μl. To recover total IRP1 binding activity, cytosolic extracts were pre-incubated for 10 min with 2-mercaptoethanol (2-ME) at 2% (v/v) final concentration, before the addition of ^{32}P-labelled IRE RNA. Unbound RNA was digested for 10 min with 1 U RNase T_1 (Roche), and non-specific RNA–protein interactions were displaced by the addition of 5 mg/ml heparin for 10 min. RNA–protein complexes were separated on 6% non-denaturing polyacrylamide gel for 2 h at 200 V. After electrophoresis, the gel was dried and autoradiographed at −80 °C. The IRPs–IRE complexes were quantified with a GS-800 imaging densitometer (Bio-Rad). Concerning IRP1, the results are expressed as the percentage of RNA-binding activity versus 2-mercaptoethanol treated samples; about IRP2 binding activity, results are expressed as percentage of untreated cells.

2.5. Western blot analysis

Samples containing 50–100 μg of proteins were denatured, separated on a 12% (for ferritin) or 8% (for IRP1, IRP2, TfR-1 and DMT-1) SDS-polyacrylamide gel and electro-transferred onto a nitrocellulose membrane (Amersham Biosciences, Little Chalfont, Buckinghamshire, UK) using a Bio-Rad Transblot (Bio-Rad). Proteins were visualized on the filters by reversible staining with Ponceau-S solution and destained in PBS. Membranes were blocked at room temperature in milk buffer [1× PBS, 5-10% (w/v) non-fat dry milk, 0.2% (v/v) Tween-20] and then incubated at 4 °C overnight with 1:1000 rabbit polyclonal antibody to human ferritin (Dako Cytomation, Glostrup, Denmark), or with 1:1000 mouse monoclonal antibody to human transferrin receptor 1 (Zymed Laboratories Inc., CA), or with 1:250 goat polyclonal antibody to human IRP1 (Santa Cruz Biotechnology, Santa Cruz, CA), or with 1:250 goat polyclonal antibody to human IRP2 (Santa Cruz Biotechnology), or with 1:250 goat polyclonal antibody to human DMT-1 (Santa Cruz Biotechnology). Subsequently, the membranes were incubated for 90 min at room temperature with peroxidase-conjugated goat anti-rabbit IgG, or peroxidase-conjugated goat anti-mouse IgG + IgM, or peroxidase-conjugated rabbit anti-goat IgG (all the secondary antibodies were purchased from Jackson ImmunoResearch Laboratories, Baltimore Pike, West Grove, PA). The resulting complexes were visualized using chemiluminescence Western blotting detection reagents (ECL, Amersham Biosciences). The optical density of the bands was determined by a GS-800 imaging densitometer (Bio-Rad). Normalization of results was ensured by incubating the nitrocellulose membranes in parallel with the β-actin antibody.

2.6. RNA extraction, Northern blot and RT-PCR analyses

Total RNA was isolated from cells using TRIzol reagent (Invitrogen Life Technologies, Carlsbad, CA) as indicated in the manufacturer's instructions. The levels of TfR mRNA were evaluated by using PCR amplification of reverse-transcribed mRNA. Total RNA was reverse-transcribed into cDNA by using the random priming method and M-MLV-Reverse Transcriptase (Invitrogen). cDNA was amplified by PCR using Taq-Polymerase (Invitrogen) according to the manufacturer's instructions. The primers for TfR were 5′-CAGCCCAGCAGAAGCATTATC-3′ (forward) and GGAAGTAGCACGGAAGAAGTC-3′ (reverse); the primers for GADPH (house-keeping gene) were 5′-ACATCAAGAAGGTGGTGAAG-3′ (forward) and 5′-CTCTTGTGCTCTTGCTGG-3′ (reverse). The TfR and GADPH cDNA were co-amplified under the following conditions: a first cycle of denaturation at 94 °C for 2 min, then 35 cycles of denaturation at 94 °C for 30 s, annealing at 46 °C for 45 s, extension at 72 °C for 1 min and one additional cycle of extension at 72 °C for 8 min. The PCR products were run on 1% agarose gel and stained with ethidium bromide. The intensities of the bands were quantified and values normalized to GADPH levels.

For Northern blots analysis, 15 μg of total RNA was fractionated on a 1.5% agarose denaturing formaldehyde gel and then transferred to Hybond-N^+ filter (Amersham Biosciences). The hybridization was performed for 18 h at 65 °C in 0.5 M sodium phosphate buffer, pH 7.2, 1 mM EDTA, pH 8.0, 7% (w/v) SDS. The filters were washed in 50 mM sodium phosphate buffer, pH 7.2, 1% (w/v) SDS at 65 °C, and then autoradiographed at −80 °C with an intensifying screen. A cDNA fragment corresponding to human H-ferritin, was ^{32}P-radiolabeled using the random priming method (Amersham Biosciences).

2.7. Cellular labile iron pool (LIP) evaluation

The cellular labile iron content was estimated by a fluorimetric assay using the metal-sensitive probe calcein (CA) [47] and the strong membrane-permeant iron chelator SIH (salicylaldehyde isonicotinoyl hydrazone), generously provided by Prof. Prem Ponka (McGill University, Montreal, QC, Canada). After incubation for 12, 24 and 48 h with 0.01, 1, or 100 pg/ml of TCDD, MDBK cells, plated at a density of 1.5×10^3 cells/well, were loaded with 0.5 μM CA-AM (calcein-acetomethoxy, Molecular Probes, Invitrogen, Eugene, OR) for 45 min at 37 °C in calcium- and bicarbonate-free modified Krebs Henseleit buffer (KHB), consisting of 20 mM HEPES, pH 7.4, 119 mM NaCl, 4.9 mM KCl, 0.96 mM KH_2PO_4 and 5 mM glucose. CA-AM rapidly penetrates across the plasma membrane and is intracellularly hydrolysed to release free CA. After loading, the cultures were washed of excess CA-AM two times with KHB. Cellular CA fluorescence was recorded in a Perkin Elmer microplate reader (Perkin Elmer LS 55 Luminescence Spectrometer, Beaconsfield, UK) using a filter combination with an excitation wavelength of 485 nm and an emission wavelength of 530 nm (slits 5 nm). Cell cultures without CA-AM were used as blank to correct non-specific autofluorescence. Trypan blue was added in all experiments to eliminate extracellular fluorescence. Once hydrolyzed, calcein becomes trapped in the cytoplasm and emits intense green fluorescence. The calcein-loaded cells have a fluorescence component (ΔF) that is quenched by intracellular iron and can be revealed by addition of 100 μM SIH. The rise in fluorescence is equivalent to the change in calcein concentration or to the amount of cellular iron originally bound to CA. Thus, the changes in CA fluorescence intensity were directly proportional to the iron labile pool. To characterize the responsiveness of CA fluorescence toward different concentrations of intracellular iron, cells were preloaded with ferrous ammonium sulphate, ferric ammonium citrate or with the cell-permeable ferrous iron chelator SIH.

2.8. Statistical analysis

For the MTT assay, cell counting and LIP determination, results are expressed as mean of percentage ± standard error of the mean (SEM) of n observations respect to control cells (100%), where n represents the number of experiments performed on different days. The results were analyzed by one-way ANOVA followed by a Bonferroni post hoc test for multiple comparisons. A p-value less than 0.05 was considered significant. The densitometric data from EMSA and Western blot analysis are reported as percentage of controls ± standard error of the mean (SEM) of n observations, where n represents the number of experiments performed on different days. Statistical significance among the results was determined by the ANOVA followed by the Newman–Keuls test. A p-value less than 0.05 was considered statistically significant.

3. Results

3.1. TCDD effect on MDBK cells viability and proliferation

We analyzed the effect of TCDD exposure on MDBK cells viability and proliferation by measuring the mitochondrial redox capacity

Table 1
TCDD effect on MDBK cell viability and proliferation.

Time (h)	TCDD (pg/ml)	Cell viability (MTT assay)	Cell proliferation (cell counting)
12	0.01	100 ± 2.22[a]	111.57 ± 4.36*, [a]
	1	101.96 ± 2.04[a]	138 ± 4.76***, [a]
	100	109.26 ± 1.28[a]	157 ± 4.67***, [a]
24	0.01	104.84 ± 1.6[a]	127 ± 3.61**, [a]
	1	103.8 ± 1.9[a]	156.14 ± 2.03***, [a]
	100	122.4 ± 0.95***, [a]	177.47 ± 3.02***, [a]
48	0.01	105.4 ± 1.45[a]	118.48 ± 1.63**, [a]
	1	113.3 ± 2.43*, [a]	150.97 ± 2.09***, [a]
	100	145.6 ± 2.38***, [a]	194.99 ± 2.5***, [a]

Data are expressed as mean of percentage ± SEM of four independent experiments performed in duplicate vs. control cultures.
[a] $n = 32$.
* $p<0.05$ vs. control.
** $p<0.01$ vs. control.
*** $p<0.001$ vs. control.

with the MTT assay and by evaluation of cell number. Confluent monolayers of MDBK cells were incubated in presence of 0.01, 1 and 100 pg/ml of TCDD and then the MTT assay was performed at different times (12, 24 and 48 h). As shown in Table 1, and reported previously in another context [43], the exposure of MDBK cells to various amount of TCDD caused a consistent increase in the mitochondrial dehydrogenases reaching 145% with respect to control cells after 48 h of incubation with 100 pg/ml of TCDD. Concomitantly, the number of cells significantly increased at all concentrations of TCDD (0.01, 1, and 100 pg/ml) and at all time intervals studied (12, 24 and 48 h). Hence, the TCDD exposure determines an increase in cell proliferation and viability at all concentration and times studied.

3.2. TCDD modulates the iron regulatory proteins activity

In order to investigate the effects of TCDD exposure on cellular iron metabolism, we first analyzed the RNA-binding activity of IRPs. To this aim, MDBK cells were exposed to different concentrations of TCDD (0.01, 1 and 100 pg/ml) and then we examined at different times of incubation (1, 12, 24, 48 and 72 h) the IRPs activity on cell lysates by means of EMSA. The results revealed a divergent regulation of IRPs activity, already evident at 24 h of TCDD exposure and at the lowest dose (0.01 pg/ml) of the contaminant. Conversely, brief incubation (1 h) of cells with TCDD did not change IRPs binding capacity at all tested concentrations (data not shown). In detail, as shown in Fig. 1, TCDD did cause a significant time-dependent decrease in IRP1 RNA-binding activity, reaching about 45% with respect to control after 48 h of incubation. Prolonged treatment up to 72 h determined only very little changes on the RNA-binding activity of IRP1. TCDD effect on IRP1 activity resulted to be dose-independent.

Interestingly, the decrease in IRP1 binding activity was concomitant with an increase in IRP2 RNA-binding activity, essentially detectable after 48 h of TCDD incubation, reaching the maximum extent (~155% vs. control) almost at all used concentration. Protracted treatment up to 72 h did not modify further the RNA-binding activity of IRP2.

To determine the total amount of IRP1 RNA-binding activity, 2-mercaptoethanol (2-ME) was added to the binding reaction before the addition of ^{32}P-labelled IRE to reveal "latent" IRP1 RNA-binding activity, thus giving the total amount of IRP1 activity (100% of IRE-binding). The results suggested that TCDD interferes with IRP1 RNA-binding activity without affecting its cellular content. Moreover, the 2-ME *in vitro*

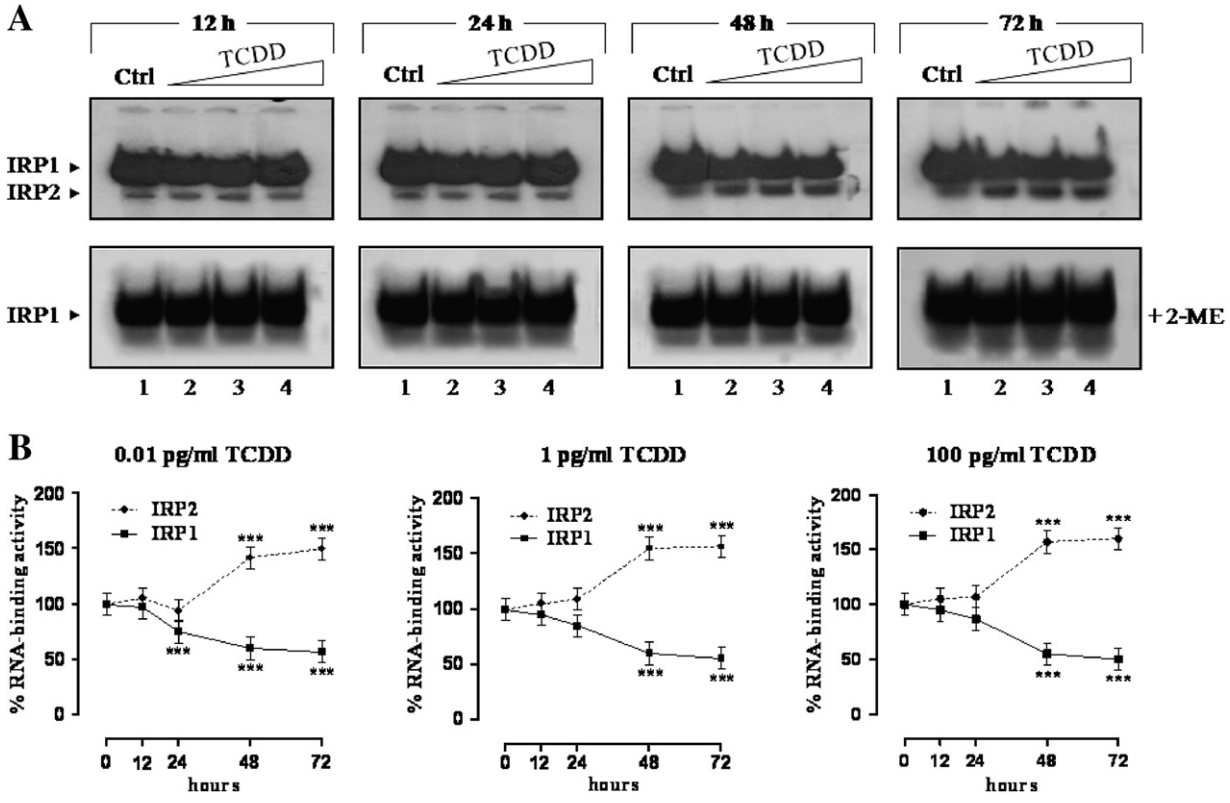

Fig. 1. TCDD effect on iron regulatory proteins activity. (A) MDBK cells were treated with different concentrations of TCDD (0.01, 1, 100 pg/ml), as indicated by numbers (2, 3, 4, respectively). Proteins were extracted and subjected to electrophoretic mobility-shift assay (EMSA). RNA band-shift assay was performed with 5 μg of cytoplasmic proteins and an excess of ^{32}P-labeled IRE probe in absence (top) or presence (bottom) of 2% 2-ME. RNA–protein complexes were separated on non-denaturing 6% polyacrylamide gel and revealed by autoradiography. The autoradiograms shown are representative of four experiments. (B) IRP1-RNA and IRP2-RNA complexes were quantified by densitometric and results of EMSA experiments performed without 2-ME were plotted in graphs as percent of the control and are the average ± SEM values of four independent experiments (solid line IRP-1; dotted line IRP-2). Graphs are distinctive depending by the indicated TCDD concentrations. ***$p<0.001$ compared with controls.

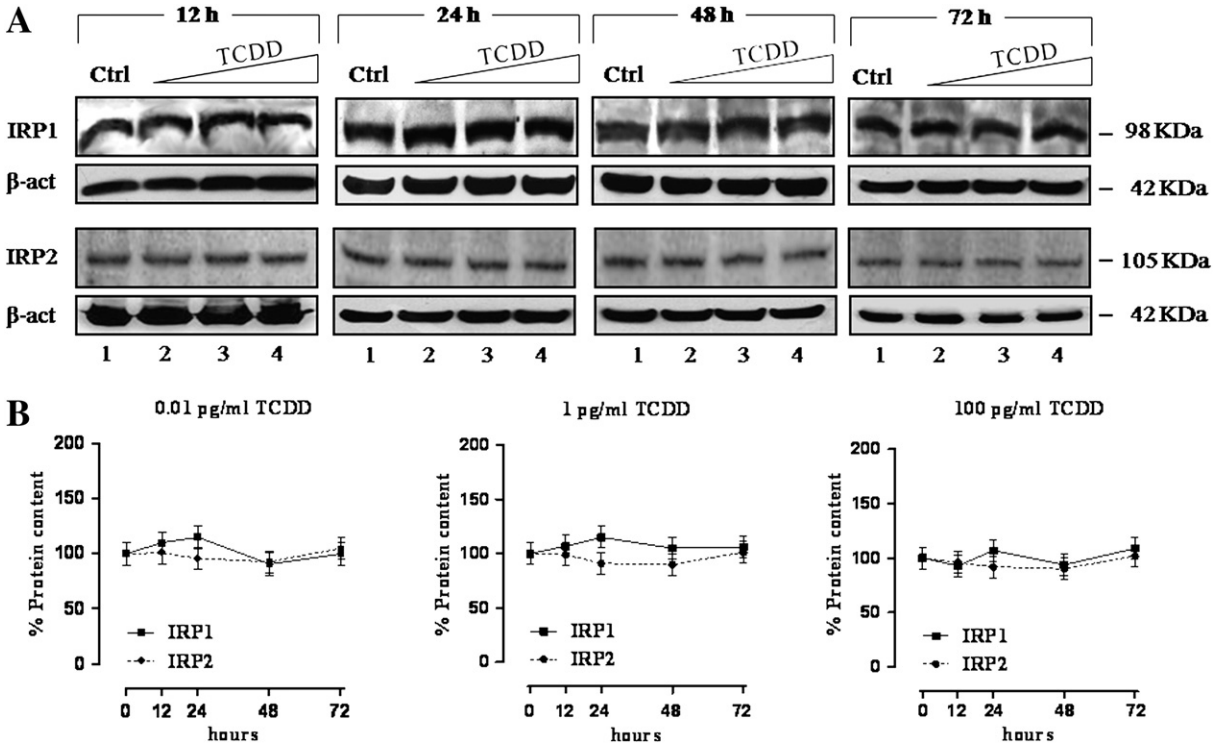

Fig. 2. (A) Western blot analysis showing the IRP1 and IRP2 protein content in MDBK cells incubated with different TCDD concentrations (0.01, 1, 100 pg/ml), as indicated by numbers (2, 3, and 4, respectively). Shown are blots representative of four independent experiments. Equal amounts of proteins (100 μg) were separated on 8% SDS-polyacrylamide gel and subjected to Western blot analysis using 1:250 dilution of IRP1 and IRP2 antisera. The anti-β-actin antibody was used to standardize the amounts of proteins in each lane. (B) After chemiluminescence, the corresponding bands were quantified by densitometric analysis and plotted in graphs as percentage of control in relation to the used TCDD concentrations, as indicated. Shown are the average ± SEM values of four independent experiments (solid line IRP-1; dotted line IRP-2).

treatment of cell extracts could result in underestimation of IRP2 activity. This is a well known and unpredictable phenomenon due to the sensitivity of IRP2 to redox status [21,48]. The modulation of IRP1 and IRP2 binding activities was not related to protein content, as resulted by the immunoblot analysis. As shown in Fig. 2, no appreciable variations in the amounts of IRP1 and IRP2 proteins were observed, suggesting that the dioxin did not affect the IRP1 and IRP2 expression.

To assess the range of IRP1 and IRP2 regulation in MDBK cells we treated the cells with iron and iron chelator, and the results are depicted in Fig. 3. As expected, exposure of cells to ferric ammonium citrate (FAC) resulted in a reduction of RNA-binding activity of both IRP1 and IRP2. Conversely, the treatment with desferrioxamine (DFO) determined an increase of RNA binding of IRP1 and the stabilization of IRP2. To monitor the response of MDBK cells to dioxin and to intracellular iron changes we exposed the cells to TCDD (1 pg/ml) for 48 h and then to FAC or DFO for the last 18 h. As shown in Fig. 3, in TCDD-treated cells the effect of iron addition or chelation is slightly quenched by the effect of TCDD.

3.3. TCDD influences TfR-1, ferritin and DMT-1 expression

To evaluate the effects of TCDD exposure on TfR-1, DMT-1 and ferritin expression in MDBK cells, we determined the levels of these proteins by Western blot analysis on lysates obtained from cells incubated for different times in presence of TCDD (0.01, 1 and 100 pg/ml). TCDD exposure remarkably and progressively increased TfR-1 expression at the cell membrane. In fact, as shown in Fig. 4, after 72 h of TCDD exposure there is evidence for a consistent, TCDD concentration-independent, increase of TfR-1 levels of about 180% with respect to control cells. TfR-1 levels were unchanged in MDBK cells after 1 h of TCDD incubation (data not shown).

Bovine kidney cell lysates showed an electrophoretic pattern in which the H- and L-ferritin subunits overlapped, as previously reported [22]. The ferritin expression showed an original biphasic response with no TCDD dose–response relationship. In fact, as depicted in Fig. 4, throughout the early phase of TCDD exposure (with the exception of 1 h of treatment wherein ferritin level did not change), ferritin protein content progressively enhanced, reaching an increase of about 1.5-fold after 24 h. In the late phase of TCDD exposure (48–72 h), ferritin considerably and rapidly decreased to about 50% of that in control cells. Furthermore, immunoblot analysis showed that DMT-1 content was almost unaffected by TCDD exposure.

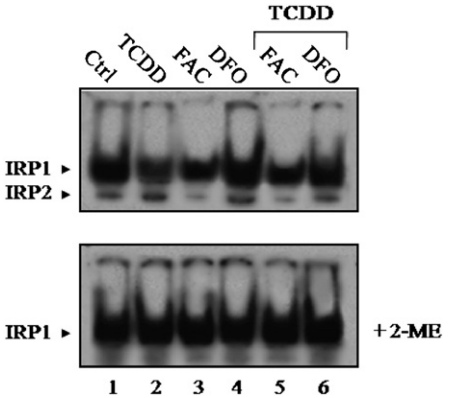

Fig. 3. Response of iron regulatory proteins activity to iron levels in epithelial-like bovine kidney cells, incubated or not with 1 pg/ml of TCDD for 48 h. For iron repletion–depletion experiments, MDBK cells were treated with 50 μg/ml ferric ammonium citrate (FAC) or with 100 μM desferrioxamine (DFO) for 18 h in absence (lanes 3 and 4) or presence (lanes 5 and 6) of 1 pg/ml TCDD. Proteins were then extracted and subjected to electrophoretic mobility-shift assay (EMSA). RNA band-shift assay was performed with 5 μg of cytoplasmic proteins and an excess of ^{32}P-labeled IRE probe in absence (top) or presence (bottom) of 2% 2-ME. RNA–protein complexes were separated on non-denaturing 6% polyacrylamide gel and revealed by autoradiography. The autoradiograms shown are representative of four experiments.

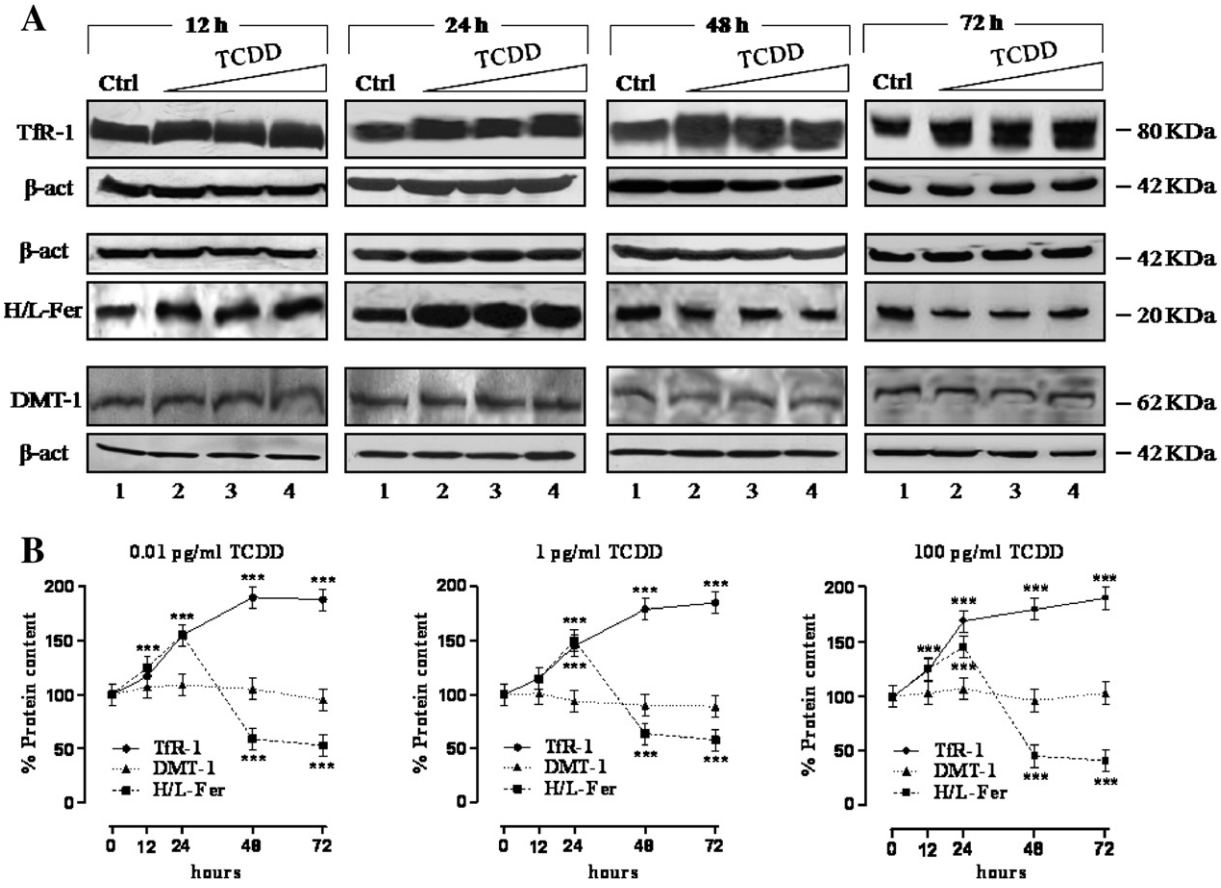

Fig. 4. (A) Western blot analysis showing the transferrin receptor-1 (TfR-1), the divalent metal transporter-1 (DMT-1), and the ferritin (H/L-Fer) levels in MDBK cells incubated with different TCDD concentrations (0.01, 1, 100 pg/ml), as indicated by numbers (2, 3, and 4, respectively). Shown are blots representative of four independent experiments. For TfR-1 content analysis, equal amounts of cytosolic lysates containing 100 μg of proteins were fractionated by 8% SDS-PAGE and subjected to Western blot analysis using 1:1000 dilution of TfR-1 antiserum. For ferritin content analysis, equal amounts of cytosolic lysates containing 100 μg of proteins were fractionated by 12% SDS-PAGE and subjected to Western blot analysis using 1:1000 dilution of ferritin antiserum. For DMT-1 level analysis, equal amounts of cytosolic lysates containing 100 μg of proteins were fractionated by 8% SDS-PAGE and subjected to Western blot analysis using 1:250 dilution of DMT-1 antiserum. The anti-β-actin antibody was used to standardize the amounts of proteins in each lane. (B) TfR-1, H/L-Fer and DMT-1 bands detected by chemiluminescence were quantified by densitometric analysis and plotted in graphs as percentage of control (solid line TfR-1; broken line ferritin; dotted line DMT-1) in relation to the used TCDD concentrations, as indicated. Shown are the average ± SEM values of four independent experiments. ***$p<0.001$ vs. control cells.

To determine whether the effect of TCDD on ferritin and TfR expression could result from a transcriptional control, we decided to analyze at 24 and 48 h the levels of TfR and ferritin mRNAs by means of RT-PCR and Northern blot analysis, respectively. Fig. 5 (panel A) shows that treatment of cells with TCDD for 24 and 48 h elicited a marked increase at all tested concentrations of TfR mRNA levels as compared to untreated cells. On the other hand exposure of cells to TCDD led to an increase in ferritin mRNA levels only in the early phase (24 h) while ferritin mRNA content remained unchanged after 48 h of TCDD exposure (see Fig. 5, panel B).

3.4. TCDD affects cellular labile iron pool (LIP)

Following TCDD exposure, the modulation of the activity and expression of the most important proteins involved in the maintenance of cellular iron homeostasis could ultimately lead to a modification of LIP extent. Therefore, to verify this hypothesis we used calcein (CA) fluorimetric assay to measure the cytosolic pool of chelatable iron in MBDK cells. This assay is based on the principle that the CA loaded into cell binds a large fraction of the free iron that is revealed by the addition of excess of the permeant iron-chelator SIH that restores CA's fluorescence. The magnitude of the chelator-mediated rise in fluorescence is proportional to the amount of CA-bound iron and therefore reflects the LIP extent. On the basis of immunoblot analysis of the proteins devoted to transport (TfR-1) and segregation (ferritin) of iron (see Fig. 4), we decided to evaluate the LIP extent between 12 and 48 h. The results derived from fluorescence intensity histograms of experiments where MBDK cells, treated for the indicated times with 0.01, 1 and 100 pg/ml of TCDD, are depicted in the Fig. 6. The LIP progressively decreased reaching the lowest level after 24 h, with a diminution of about 70% respect to control cells. Then, LIP rapidly increased reaching the maximum after 48 h (about the 150% respect to untreated cells). The variations in LIP magnitude were TCDD concentrations-independent.

4. Discussion

Dioxins are known to be a class of highly toxic and persistent environmental contaminants, among them the 2,3,7,8-tetrachlorodibenzo-*p*-dioxin (TCDD) is believed to be one of the most potent chemical toxins of current interest. One of the major TCDD *in vivo* target organ is the liver, which plays a fundamental function in iron metabolism [49]. Indeed, TCDD-induced disturbances in iron homeostasis have been reported in correlation with liver injury. Evidence is consistent with the involvement of iron metabolism genes in dioxin-induced uroporphyria and liver oxidative injury [41,42].

In the present study, we have provided the first evidence *in vitro* that exposure of mammalian cells to the toxin TCDD affects the maintenance of iron homeostasis, causing an opposite modulation of the iron regulatory proteins activity, with consequent variations in the expression of the main iron related proteins, and ultimately significant changes in the extent of the intracellular free iron pool.

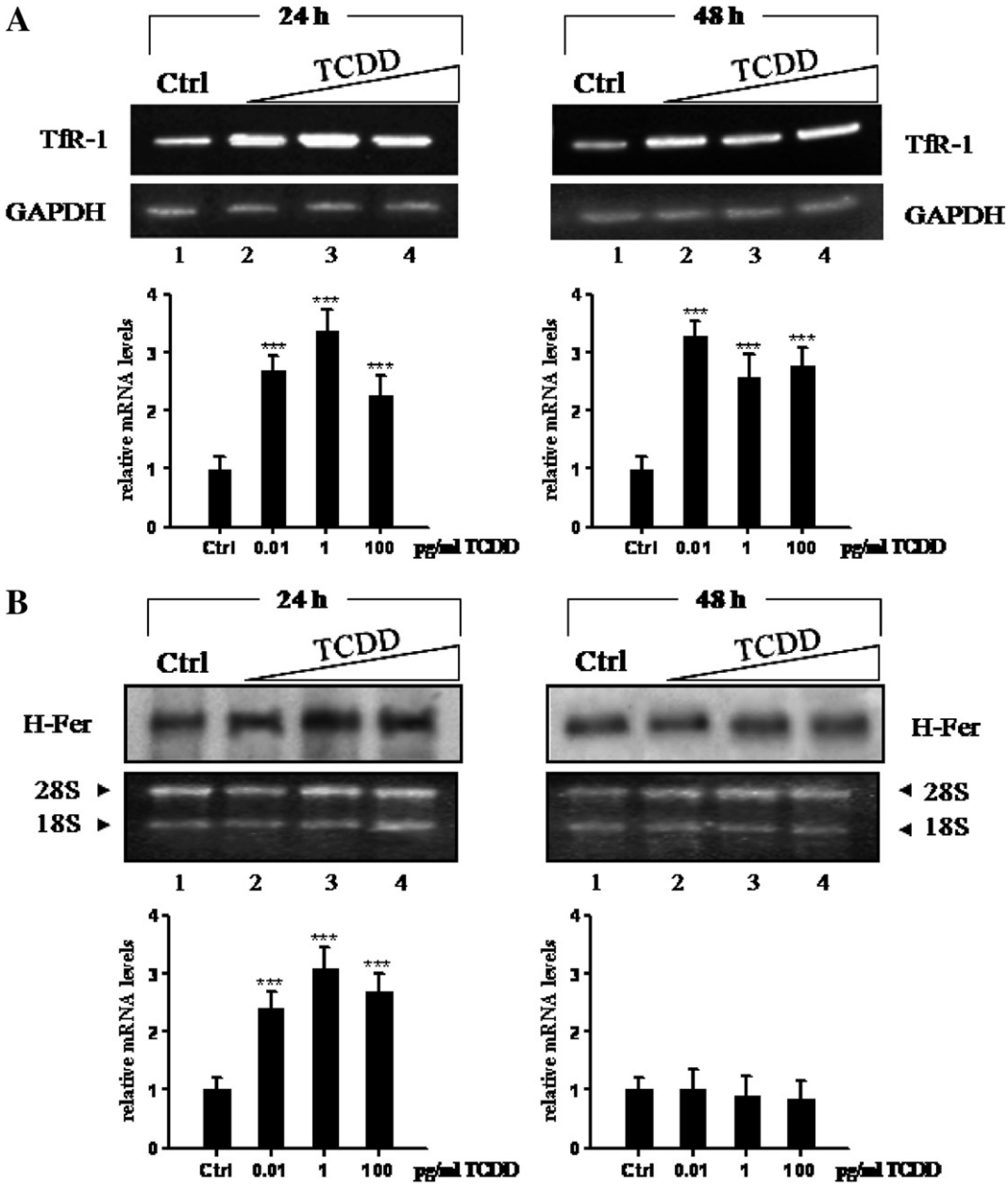

Fig. 5. TCDD effect on TfR-1 and ferritin mRNA levels in MDBK cells incubated for the indicated times with different TCDD concentrations (0.01, 1, 100 pg/ml), as showed by numbers (2, 3, and 4, respectively). (A) RT-PCR and its densitometric analysis showing TfR-1 mRNA expression. Shown are RT-PCR analysis representative of three independent experiments. Total RNA was reverse-transcribed into cDNA by using the random priming method and then cDNA was amplified by PCR using Taq-Polymerase. The TfR-1 and GADPH (house-keeping gene) cDNA were co-amplified as described in Materials and methods section. After gel staining, the bands corresponding to TfR-1 mRNAs were quantified by densitometric analysis and plotted in bar graphs as relative units showing the average ± SEM values of three independent experiments. ***$p<0.001$ vs. control cells. (B) Northern blot and its densitometric analysis showing H-ferritin (H-Fer) mRNA levels. The autoradiograms shown are representative of three independent experiments. Equal amounts (15 μg) of total cellular RNA, as revealed by ethidium bromide fluorescence of RNA gel, were hybridized to an H-ferritin cDNA ^{32}P-radiolabelled probe. The bands corresponding to H-ferritin mRNA were quantified by densitometric and the mean ± SEM of results from three experiments are plotted in bar graphs as relative units. ***$p<0.001$ vs. control cells.

We have evaluated the IRPs/IRE interactions and the results revealed that cell exposure to TCDD affects the RNA-binding capacity of both IRP1 and IRP2. Notably, in our *in vitro* experimental model TCDD interfered with iron regulatory proteins activity at a very low dose (0.01 pg/ml), suggestive of a relevant influence of dioxin in the regulation of iron metabolism. We observed a concomitant IRP1 down-regulation and IRP2 up-regulation, more evident at prolonged exposure times. These effects on IRPs activity showed a time-dependent and dose-independent profile. This phenomenon is related to the complexity of mechanisms by which many xenobiotics, such as halogenated hydrocarbons, polycyclic aromatic hydrocarbons, phthalates and pesticides, exert toxic effects [50]. Indeed, the TCDD effects on iron metabolism regulation were dose-independent, whereas the increase in mitochondrial activity and in cell proliferation were clearly dependent on the TCDD dose [43].

The treatment of MDBK cells with iron and desferrioxamine, a potent iron chelator, demonstrates that our experimental model responds to iron content variation in accordance with the well known iron regulation of IRPs. Although it appears slightly quenched, the effect of iron addition or chelation on IRPs activity was persistent following TCDD exposure. Moreover, the RNA-binding activity assays in the presence of the reducing agent 2-ME, which converts c-aconitase into the fully activated IRP1, indicate that the TCDD-dependent decrease in the IRP1 RNA-binding activity is correlated with an increase of c-aconitase form.

Interestingly, no appreciable variations in cellular IRP1 and IRP2 content occurred, thus suggesting that TCDD modulates RNA-binding

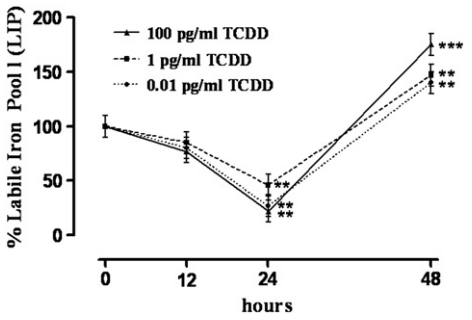

Fig. 6. LIP extent following TCDD exposure (0.01,1, 100 pg/ml) in MDBK cells estimated for the indicated times with the CA fluorescent method. Cell cultures were loaded with CA using acetomethoxyl-calcein, and fluorescence was measured before and after the addition of 100 μM permeant iron chelator SIH. Shown are the average ± SEM ($n = 6$) values of three independent experiments plotted in a graph as percent of control cultures. $^{**}p < 0.01$ vs. control cells; $^{***}p < 0.001$ vs. control cells.

activity without affecting the protein expression. Bearing in mind the accepted model that IRP2 is either functional or degraded, the data concerning the increased IRP2 activity observed in the RNA-binding experiments and the results of IRP2 expression seem to be apparently contradictory, probably because of the low sensitivity of the IRP2 immunoblot experiments.

The observed IRPs regulation by TCDD could be a consequence of a toxic process or a signaling pathway to cope with oxidative stress [41]. The decrease in IRP1 binding activity is partly consistent with previous results on livers from TCDD-susceptible mice, showing a depression of IRP1, due to a down-regulation of protein expression or to an IRE-binding capacity inactivation [41]. Since the toxic and biochemical effects of TCDD are mainly if not exclusively dependent on its binding to the cytoplasmic Aryl hydrocarbon Receptor (AhR), it appears likely that the AhR could also play a role in the TCDD-dependent regulation of iron metabolism. It is known that dioxins interfere with the endocrine system acting as Endocrine Disrupting Chemicals (EDC), hence modifying the regulation of dynamic cellular processes [30,34]. By multiple mechanisms based on AhR-Nuclear Receptors crosstalk, EDCs exert numerous hormone disruptive activities [51]. In fact, there is evidence showing a crosstalk between the estrogen receptors (ERs) and AhR that leads to inhibition of estrogenic signaling. The anti-estrogenic influence of TCDD on ER signaling is well documented, even though the mechanism is not fully characterized [52,53]. Recently, we have reported that the molecular mechanism governing the regulation of ferritin and TfR-1 gene expression by estrogen is based on changes in the IRE binding activity of the IRPs. In particular, we showed a reduced IRP1 binding activity in an *in vivo* model of estrogen deficiency, suggestive of a possible hormone-dependent functional regulation of the IRP1 IRE-binding activity [23]. Accordingly, the reduced IRP1 activity herein described following the dioxin exposure could be correlated to the TCDD anti-estrogenic effect.

One intriguing finding is the concomitant IRP2 up-regulation following the dioxin exposure. The enhanced activity of IRP2, when IRP1 activity is low, could be due to compensatory mechanisms within iron homeostasis regulation as a consequence of protein over-expression or/and a misregulation of the intricate E3 ubiquitin ligase machinery devoted to IRP2 proteasomal degradation. In mammals, kidney is one of the tissues in which IRP1 is most highly expressed, contributing significantly to regulation of iron metabolism [54]. Nevertheless, in several tissues, as well as kidney, loss of IRP1-binding activity does not lead to misregulation of iron metabolism, because IRP2 levels increase in compensation [55]. However, the possibility cannot be excluded that IRP2 activity may be subjected to as yet unidentified regulatory mechanism induced by TCDD.

Modulation of IRPs binding activity would ultimately lead to changes in iron-related protein expression profiling. It is well known that at post-transcriptional level, the up-regulation of IRPs RNA-binding activity leads to an increased TfR-1 mRNA translation and to a simultaneous decreased ferritin mRNA translation. In MDBK cells exposed to TCDD a marked enhancement of TfR-1 expression was observed, that predictably is associated with enhanced iron uptake, whereas the cellular DMT-1 levels appear unchanged, suggesting a minor role of this transporter in the control of iron flux in consequence of the dioxin effect. Concerning ferritin expression, TCDD exposure determined an original biphasic response with a progressive increase in ferritin content until 24 h, and then a rapid and substantial reduction in its content, clearly detectable at 48 and 72 h of exposure. The increased expression of TfR-1 is dependent by a coupled transcriptional and post-transcriptional regulation, as also demonstrated through enhanced TfR-1 mRNA steady-state levels (see Fig. 5, panel A). As regards the biphasic behaviour of ferritin, the protein increase after 24 h of treatment is consistent with an increase of steady-state levels of ferritin mRNA induced by TCDD (see Fig. 5, panel B), whereas the reduced levels observed after prolonged TCDD exposure (48–72 h) appear correlated to the increased IRP2 binding activity without concurrent significant variations of mRNA steady-state levels. Although it is known that in kidney IRP1 mainly contributes to regulation of iron metabolism, it is feasible that IRP2 can act as the effector of cellular iron homeostasis when the TCDD exposure is prolonged to 72 h and IRP1 fails in controlling iron sense. To our knowledge, the present results are the first demonstration of a divergent response of IRP1 and IRP2 to TCDD toxicity.

The simultaneous changes on ferritin content and TfR-1 induction by TCDD exposure could impair cellular iron homeostasis, ultimately leading to important alterations of the labile iron pool (LIP) extent. LIP, the portion of free cellular iron, is mainly localized but not exclusively in the cytosol and constitutes the catalytic and redox-active iron. The level of the pool must be maintained within a restricted range that meets the cell's requirements for iron but prevents excess from developing cellular oxidative damage [56]. Evaluation of the LIP magnitude in MDBK cells exposed to TCDD indicated important fluctuations within the pool, largely in relation to the expression of the iron-withdrawing protein ferritin, the major controller of the iron pool. In fact, the TCDD-dependent decrease of cellular ferritin content, coupled with TfR-1 induction detected after 48 h of treatment, was associated with enhanced LIP level. The result that LIP levels rapidly and markedly changed following TCDD exposure strongly supports the hypothesis that dioxin causes alterations in the maintenance of cellular iron homeostasis. Interestingly, although iron repletion would be sufficient to degrade IRP2 via the E3 ligase ubiquitin proteasomal pathway, IRP2 remains active, a finding that reinforces the concept that in our experimental model this protein is predominant in the control of cellular iron metabolism.

In correlation to the enlarged iron pool at 48 h, we have observed that cell viability and cell number significantly increase in presence of TCDD in a dose-dependent manner. Hence, since important iron requirement changes occur during the regulation of cell growth, it is not surprising that the dioxin-dependent iron metabolism deregulation, herein described, may affect cell-fate decision. Deregulation of cell proliferation/differentiation processes induced by dioxin coupled to an iron excess could be ultimately associated to the neoplastic transformation of the cell and to cancer development [57,58]. This is supported by a recent report that demonstrates a pro-oncogenic activity for IRP2 to induce the growth of tumor xenografts [59].

In conclusion, altogether these observations warrant a reconsideration of iron role in TCDD-induced toxicity and highlight a central connection among the exposure to dioxins, the fine regulation of iron metabolism and the control of dynamic cellular processes.

Acknowledgments

The authors express their gratitude to Professor Prem Ponka (McGill University, Montreal, QC, Canada) for having kindly provided the iron chelator SIH.

References

[1] J. Beard, Iron deficiency alters brain development and functioning, J. Nutr. 133 (2003) 1468S–1472S.
[2] S.K. Nelson, J.M. McCord, Iron, oxygen radicals, and disease, Adv. Mol. Cell. Biol. 25 (1998) 157–183.
[3] S. Toyokuni, Iron-induced carcinogenesis: the role of redox regulation, Free Radic. Biol. Med. 20 (1996) 553–566.
[4] E. Nemeth, M.S. Tuttle, J. Powelson, M.B. Vaughn, A. Donovan, D.M. Ward, T. Ganz, J. Kaplan, Hepcidin regulates cellular iron efflux by binding to ferroportin and inducing its internalization, Science 306 (2004) 2090–2093.
[5] E. Nemeth, T. Ganz, The role of hepcidin in iron metabolism, Acta Haematol. 122 (2009) 78–86.
[6] M.W. Hentze, M.U. Muckenthaler, N.C. Andrews, Balancing acts: molecular control of mammalian iron metabolism, Cell 117 (2004) 285–297.
[7] K. Pantopoulos, Iron metabolism and the IRE/IRP regulatory system: an update, Ann. N. Y. Acad. Sci. 1012 (2004) 1–13.
[8] T.A. Rouault, The role of iron regulatory proteins in mammalian iron homeostasis and disease, Nat. Chem. Biol. 2 (2006) 406–414.
[9] M.U. Muckenthaler, B. Galy, M.W. Hentze, Systemic iron homeostasis and the iron-responsive element/iron-regulatory protein (IRE/IRP) regulatory network, Annu. Rev. Nutr. 28 (2008) 197–213.
[10] M.L. Wallander, E.A. Leibold, R.S. Eisenstein, Molecular control of vertebrate iron homeostasis by iron regulatory proteins, Biochim. Biophys. Acta 1763 (2006) 668–689.
[11] J.B. Fishman, J.B. Rubin, J.V. Handrahan, J.R. Connor, R.E. Fine, Receptor mediated transcytosis of transferrin across the blood-brain barrier, J. Neurosci. Res. 18 (1987) 299–304.
[12] M.P. Mims, J.T. Prchal, Divalent metal transporter 1, Hematology 10 (2005) 339–345.
[13] N. Aziz, H.N. Munro, Iron regulates ferritin mRNA translation through a segment of its 5′ untranslated region, Proc. Natl Acad. Sci. USA 84 (1987) 8478–8482.
[14] M.C. Kennedy, L. Mende-Mueller, G.A. Blondin, H. Beinert, Purification and characterization of cytosolic aconitase from beef liver and its relationship to the iron-responsive element binding protein, Proc. Natl Acad. Sci. USA 89 (1992) 11730–11734.
[15] A.A. Salahudeen, J.W. Thompson, J.C. Ruiz, H.W. Ma, L.N. Kinch, Q. Li, N.V. Grishin, R.K. Bruick, An E3 ligase possessing an iron-responsive hemerythrin domain is a regulator of iron homeostasis, Science 326 (2009) 722–726.
[16] A.A. Vashisht, K.B. Zumbrennen, X. Huang, D.N. Powers, A. Durazo, D. Sun, N. Bhaskaran, A. Persson, M. Uhlen, O. Sangfelt, C. Spruck, E.A. Leibold, J.A. Wohlschlegel, Control of iron homeostasis by an iron-regulated ubiquitin ligase, Science 326 (2009) 718–721.
[17] K. Pantopoulos, S. Mueller, A. Atzberger, W. Ansorge, W. Stremmel, M.W. Hentze, Differences in the regulation of iron regulatory protein-1 (IRP1) by extra- and intra-cellular oxidative stress, J. Biol. Chem. 272 (1997) 9802–9808.
[18] J.C. Drapier, H. Hirling, J. Wietzerbin, P. Kaldy, L.C. Kühn, Biosynthesis of nitric oxide activates iron regulatory factor in macrophages, EMBO J. 12 (1993) 3643–3649.
[19] N.M. Brown, S.A. Anderson, D.W. Steffen, T.B. Carpenter, M.C. Kennedy, W.E. Walden, R.S. Eisenstein, Novel role of phosphorylation in Fe–S cluster stability revealed by Phosphomimetic mutation at Ser-138 of iron regulatory protein 1, Proc. Natl Acad. Sci. USA 95 (1998) 15235–15240.
[20] E.G. Meyron-Holtz, M.C. Ghosh, T.A. Rouault, Mammalian tissue oxygen levels modulate iron-regulatory protein activities in vivo, Science 306 (2004) 2087–2090.
[21] C. Irace, A. Scorziello, C. Maffettone, G. Pignataro, C. Matrone, A. Adornetto, R. Santamaria, L. Annunziato, A. Colonna, Divergent modulation of iron regulatory proteins and ferritin biosynthesis by hypoxia/reoxygenation in neurons and glial cells, J. Neurochem. 95 (2005) 1321–1331.
[22] C. Maffettone, L. De Martino, C. Irace, R. Santamaria, U. Pagnini, G. Iovane, A. Colonna, Expression of iron-related proteins during infection by bovine herpes virus type-1, J. Cell. Biochem. 104 (2008) 213–223.
[23] G. Mattace Raso, C. Irace, E. Esposito, C. Maffettone, A. Iacono, A. Di Pascale, R. Santamaria, A. Colonna, R. Meli, Ovariectomy and estrogen treatment modulate iron metabolism in rat adipose tissue, Biochem. Pharmacol. 78 (2009) 1001–1007.
[24] M. Festa, A. Colonna, C. Pietropaolo, A. Ruffo, Oxalomalate, a competitive inhibitor of aconitase, modulates the RNA-binding activity of iron-regulatory proteins, Biochem. J. 348 (2000) 315–320.
[25] R. Santamaria, C. Irace, M. Festa, C. Maffettone, A. Colonna, Induction of ferritin expression by oxalomalate, Biochim. Biophys. Acta 1691 (2004) 151–159.
[26] R. Santamaria, M.A. Bevilacqua, C. Maffettone, C. Irace, B. Iovine, A. Colonna, Induction of H-ferritin synthesis by oxalomalate is regulated at both the transcriptional and post-transcriptional levels, Biochim. Biophys. Acta 1763 (2006) 815–822.
[27] A. Schecter, L. Birnbaum, J.J. Ryan, J.D. Constable, Dioxins: an overview, Environ. Res. 101 (2006) 419–428.
[28] F. Santelli, F. Boscaino, D. Cautela, D. Castaldo, A. Malorni, Determination of polychlorinated dibenzo-*p*-dioxins (PCDDs), polychlorinated dibenzo-*p*-furans (PCDFs) and polychlorinated biphenyls (PCBs) in buffalo milk and mozzarella cheese, Eur. Food Res. Technol. 223 (2006) 51–56.
[29] G. Diletti, L. Torreti, M.R. De Massis, G. Migliorati, G. Scortichini, A case of milk contamination by PCDD/Fs in Italy: analytical levels and contamination source identification, Organohalogen Compouds 64 (2003) 1–4.
[30] P.K. Mandal, Dioxin: a review of its environmental effects and its aryl hydrocarbon receptor biology, J. Comp. Physiol. B 175 (2005) 221–230.
[31] S. Knerr, D. Schrenk, Carcinogenicity of 2,3,7,8-tetrachlorodibenzo-*p*-dioxin in experimental models, Mol. Nutr. Food Res. 50 (2006) 897–907.
[32] R. Pohjanvirta, J. Tuomisto, Short-term toxicity of 2,3,7,8-tetrachlorodibenzo-*p*-dioxin in laboratory animals: effects, mechanisms, and animal models, Pharmacol. Rev. 46 (1994) 483–549.
[33] D. Consonni, A.C. Pesatori, C. Zocchetti, R. Sindaco, L.C. D'Oro, M. Rubagotti, P.A. Bertazzi, Mortality in a population exposed to dioxin after the Seveso, Italy, accident in 1976: 25 years of follow-up, Am. J. Epidemiol. 167 (2008) 847–858.
[34] P. Mocarelli, P.M. Gerthoux, D.G. Patterson, S. Milani, G. Limonta, M. Bertona, S. Signorini, P. Tramacere, L. Colombo, C. Crespi, P. Brambilla, C. Sarto, V. Carreri, E.J. Sampson, W.E. Turner, L.L. Needham, Dioxin exposure, from infancy through puberty, produces endocrine disruption and affects human semen quality, Environ. Health Perspect. 116 (2008) 70–77.
[35] K.W. Bock, C. Köhle, Ah receptor: dioxin-mediated toxic responses as hints to deregulated physiologic functions, Biochem. Pharmacol. 72 (2006) 393–404.
[36] S. Ray, H.I. Swanson, Activation of the aryl hydrocarbon receptor by TCDD inhibits senescence: a tumor promoting event? Biochem. Pharmacol. 77 (2009) 681–688.
[37] F. Ohtake, A. Baba, I. Takada, M. Okada, K. Iwasaki, H. Miki, S. Takahashi, A. Kouzmenko, K. Nohara, T. Chiba, Y. Fujii-Kuriyama, S. Kato, Dioxin receptor is a ligand-dependent E3 ubiquitin ligase, Nature 446 (2007) 562–566.
[38] K.W. Bock, C. Köhle, The mammalian aryl hydrocarbon (Ah) receptor: from mediator of dioxin toxicity toward physiological functions in skin and liver, Biol. Chem. 390 (2009) 1225–1235.
[39] Z.A. al-Bayati, Z.Z. Wahba, S.J. Stohs, 2,3,7,8-Tetrachlorodibenzo-*p*-dioxin (TCDD)-induced alterations in lipid peroxidation, enzymes, and divalent cations in rat testis, Xenobiotica 18 (1988) 1281–1289.
[40] Z.Z. Wahba, Z.A. al-Bayati, S.J. Stohs, Effect of 2,3,7,8-tetrachlorodibenzo-*p*-dioxin on the hepatic distribution of iron, copper, zinc, and magnesium in rats, J. Biochem. Toxicol. 3 (1988) 121–129.
[41] A.G. Smith, B. Clothier, S. Robinson, M.J. Scullion, P. Carthew, R. Edwards, J. Luo, C.K. Lim, M. Toledano, Interaction between iron metabolism and 2,3,7,8-tetrachlorodibenzo-*p*-dioxin in mice with variants of the Ahr gene: a hepatic oxidative mechanism, Mol. Pharmacol. 53 (1998) 52–61.
[42] R. Davies, B. Clothier, S.W. Robinson, R.E. Edwards, P. Greaves, J. Luo, T.W. Gant, T. Chernova, A.G. Smith, Essential role of the AH receptor in the dysfunction of heme metabolism induced by 2,3,7,8-tetrachlorodibenzo-*p*-dioxin, Chem. Res. Toxicol. 21 (2008) 330–340.
[43] F. Fiorito, U. Pagnini, L. De Martino, S. Montagnaro, R. Ciarcia, S. Florio, M. Pacilio, A. Fucito, A. Rossi, G. Iovane, A. Giordano, 2,3,7,8-Tetrachlorodibenzo-*p*-dioxin increases bovine herpesvirus type-1 (BHV-1) replication in Madin–Darby Bovine Kidney (MDBK) cells in vitro, J. Cell. Biochem. 103 (2008) 221–233.
[44] F. Fiorito, G. Marfè, E. De Blasio, G.E. Granato, M. Tafani, L. De Martino, S. Montagnaro, S. Florio, U. Pagnini, 2,3,7,8-Tetrachlorodibenzo-*p*-dioxin regulates bovine herpesvirus type 1 induced apoptosis by modulating Bcl-2 family members, Apoptosis 13 (2008) 1243–1252.
[45] F. Fiorito, G. Marfè, G.E. Granato, R. Ciarcia, E. De Blasio, M. Tafani, S. Florio, L. De Martino, G. Muzi, U. Pagnini, A. Giordano, 2,3,7,8-Tetrachlorodibenzo-*p*-dioxin modifies expression and nuclear/cytosolic localization of bovine herpesvirus 1 immediate-early protein (bICP0) during infection, J. Cell. Biochem. 111 (2) (2010) 333–342.
[46] M. Festa, G. Ricciardelli, G. Mele, C. Pietropaolo, A. Ruffo, A. Colonna, Over-expression of H ferritin and up-regulation of iron regulatory protein genes during differentiation of 3T3-L1 pre-adipocytes, J. Biol. Chem. 275 (2000) 36708–36712.
[47] W. Breuer, S. Epsztejn, P. Millgram, Z.I. Cabantchik, Transport of iron and other transition metals into cells as revealed by a fluorescent probe, Am. J. Physiol. 268 (1995) 1354–1361.
[48] C. Bouton, H. Hirling, J.C. Drapier, Redox modulation of iron regulatory proteins by peroxynitrite, J. Biol. Chem. 272 (1997) 19969–19975.
[49] N. Sharma, J. Butterworth, B.T. Cooper, C. Tselepis, T.H. Iqbal, The emerging role of the liver in iron metabolism, Am. J. Gastroenterol. 100 (2005) 201–206.
[50] A.C. Gore, J.J. Heindel, R.T. Zoeller, Endocrinology 147 (2006) S1–S3.
[51] S. Safe, M. Wormke, I. Samudio, Mechanisms of inhibitory aryl hydrocarbon receptor–estrogen receptor crosstalk in human breast cancer cells, J. Mammary Gland Biol. Neoplasia 5 (2000) 295–306.
[52] S. Safe, M. Wormke, Inhibitory aryl hydrocarbon receptor–estrogen receptor alpha cross-talk and mechanisms of action, Chem. Res. Toxicol. 16 (2003) 807–816.
[53] E. Swedenborg, I. Pongratz, AhR and ARNT modulate ER signaling, Toxicology 268 (2010) 132–138.
[54] D. Zhang, E. Meyron-Holtz, T.A. Rouault, Renal iron metabolism: transferrin iron delivery and the role of iron regulatory proteins, J. Am. Soc. Nephrol. 18 (2007) 401–406.
[55] E.G. Meyron-Holtz, M.C. Ghosh, K. Iwai, T. LaVaute, X. Brazzolotto, U.V. Berger, W. Land, H. Ollivierre-Wilson, A. Grinberg, P. Love, T.A. Rouault, Genetic ablations of iron regulatory proteins 1 and 2 reveal why iron regulatory protein 2 dominates iron homeostasis, EMBO J. 23 (2004) 386–395.
[56] M. Kruszewski, Labile iron pool: the main determinant of cellular response to oxidative stress, Mutat. Res. 531 (2003) 81–92.
[57] C.J. Portier, Endocrine dismodulation and cancer, Neuro Endocrinol. Lett. 23 (2002) 43–47.
[58] S. Toyokuni, Role of iron in carcinogenesis: cancer as a ferrotoxic disease, Cancer Sci. 100 (2009) 9–16.
[59] C. Maffettone, G. Chen, I. Drozdov, C. Ouzounis, K. Pantopoulos, Tumorigenic properties of iron regulatory protein 2 (IRP2) mediated by its specific 73-amino acids insert, PLoS ONE 5 (4) (2010) e10163.